Research Article | Vol. 7, No. 8 | 1 Aug 2017 | OPTICAL MATERIALS EXPRESS 2727
Optical Materials EXPRESS

Tunability of indium tin oxide materials for mid-infrared plasmonics applications

YU WANG,[1] ADAM C. OVERVIG,[2] SAJAN SHRESTHA,[2] RAN ZHANG,[3] REN WANG,[1] NANFANG YU,[2] AND LUCA DAL NEGRO[1,3,*]

[1]*Department of Electrical and Computer Engineering and Photonics Center, Boston University, 8 Saint Mary's Street Boston, MA 02215, USA*
[2]*Department of Applied Physics and Applied Mathematics, Columbia University, New York, NY, USA*
[3]*Division of Materials Science and Engineering, Boston University, 15 Saint Mary's Street, Brookline, MA 02446, USA*
[*]*dalnegro@bu.edu*

Abstract: Transparent conductive oxides (TCOs) have emerged as alternative plasmonic materials in recent years to replace noble metals. The advantages of TCOs include CMOS compatibility, tunability of optical and structural properties, and reduced losses. In this work, we demonstrate how post-deposition annealing of indium tin oxide (ITO) films in oxygen atmosphere allows for tuning their optical dispersion properties to the mid-infrared spectral range while simultaneously reducing their absorption losses. In particular, we show a materials strategy that extends the epsilon-near-zero (ENZ) point of ITO from the near-infrared to the mid-infrared range. This is demonstrated by fabricating periodic arrays of ITO discs of varying diameters and characterizing their plasmonic resonances in the mid-infrared range from $\lambda = 5$ to 10 μm. The developed ITO plasmonic structures pave the way to the development of novel infrared active devices for sensing and spectroscopy on a silicon-compatible platform.

OCIS codes: (160.3918) Metamaterials; (160.4236) Nanomaterials; (250.5403) Plasmonics.

References and links

1. G. V. Naik and A. Boltasseva, "Semiconductors for plasmonics and metamaterials," Phys. Status Solidi Rapid Res. Lett. **4**(10), 295–297 (2010).
2. G. V. Naik and A. Boltasseva, "A comparative study of semiconductor-based plasmonic metamaterials," Metamaterials (Amst.) **5**(1), 1–7 (2011).
3. P. R. West, S. Ishii, G. V. Naik, N. K. Emani, V. M. Shalaev, and A. Boltasseva, "Searching for better plasmonic materials," Laser Photonics Rev. **4**(6), 795–808 (2010).
4. S. H. Brewer and S. Franzen, "Optical properties of indium tin oxide and fluorine-doped tin oxide surfaces: Correlation of reflectivity, skin depth, and plasmon frequency with conductivity," J. Alloys Compd. **338**(1-2), 73–79 (2002).
5. S. H. Brewer and S. Franzen, "Calculation of the electronic and optical properties of indium tin oxide by density functional theory," Chem. Phys. **300**(1-3), 285–293 (2004).
6. S. H. Brewer and S. Franzen, "Indium tin oxide plasma frequency dependence on sheet resistance and surface adlayers determined by reflectance FTIR spectroscopy," J. Phys. Chem. B **106**(50), 12986–12992 (2002).
7. S. Franzen, "Surface plasmon polaritons and screened plasma absorption in indium tin oxide compared to silver and gold," J. Phys. Chem. C **112**(15), 6027–6032 (2008).
8. Y. Wang, A. Capretti, and L. Dal Negro, "Wide tuning of the optical and structural properties of alternative plasmonic materials," Opt. Mater. Express **5**(11), 2415 (2015).
9. G. V. Naik, J. L. Schroeder, X. Ni, A. V. Kildishev, T. D. Sands, and A. Boltasseva, "Titanium nitride as a plasmonic material for visible and near-infrared wavelengths," Opt. Mater. Express **2**(4), 478 (2012).
10. G. V. Naik, V. M. Shalaev, and A. Boltasseva, "Alternative plasmonic materials: Beyond gold and silver," Adv. Mater. **25**(24), 3264–3294 (2013).
11. G. V. Naik, J. Kim, and A. Boltasseva, "Oxides and nitrides as alternative plasmonic materials in the optical range [Invited]," Opt. Mater. Express **1**(6), 1090 (2011).
12. J. F. Wager, "Applied physics. Transparent electronics," Science **300**(5623), 1245–1246 (2003).
13. X. Jiang, F. L. Wong, M. K. Fung, and S. T. Lee, "Aluminum-doped zinc oxide films as transparent conductive electrode for organic light-emitting devices," Appl. Phys. Lett. **83**(9), 1875–1877 (2003).
14. A. Capretti, Y. Wang, N. Engheta, and L. Dal Negro, "Enhanced third- harmonic generation in Si-compatible epsilon-near-zero ITO nanolayers," Opt. Lett. **40**(7), 1500 (2015).

#295386 https://doi.org/10.1364/OME.7.002727
Journal © 2017 Received 5 May 2017; revised 27 Jun 2017; accepted 27 Jun 2017; published 6 Jul 2017

Optical Materials EXPRESS

15. A. Capretti, Y. Wang, N. Engheta, and L. Dal Negro, "Comparative Study of Second-Harmonic Generation from Epsilon-Near-Zero Indium Tin Oxide and Titanium Nitride Nanolayers Excited in the Near-Infrared Spectral Range," ACS Photonics **2**(11), 1584–1591 (2015).
16. M. Z. Alam, I. De Leon, and R. W. Boyd, "Large optical nonlinearity of indium tin oxide in its epsilon-near-zero region," Science **352**(6287), 795–797 (2016).
17. H. Zhao, Y. Wang, A. Capretti, L. Dal Negro, and J. Klamkin, "Broadband Electroabsorption Modulators Design Based on Epsilon-Near-Zero Indium Tin Oxide," IEEE J. Sel. Top. Quantum Electron. **21**, 1–7 (2015).
18. V. J. Sorger, N. D. Lanzillotti-Kimura, R.-M. Ma, and X. Zhang, "Ultra-compact silicon nanophotonic modulator with broadband response," Nanophotonics **1**(1), 1–6 (2012).
19. E. Feigenbaum, K. Diest, and H. A. Atwater, "Unity-order index change in transparent conducting oxides at visible frequencies," Nano Lett. **10**(6), 2111–2116 (2010).
20. N. Kinsey, C. DeVault, J. Kim, M. Ferrera, V. M. Shalaev, and A. Boltasseva, "Epsilon-near-zero Al-doped ZnO for ultrafast switching at telecom wavelengths," Optica **2**(7), 616–622 (2015).
21. G. V. Naik, B. Saha, J. Liu, S. M. Saber, E. A. Stach, J. M. Irudayaraj, T. D. Sands, V. M. Shalaev, and A. Boltasseva, "Epitaxial superlattices with titanium nitride as a plasmonic component for optical hyperbolic metamaterials," Proc. Natl. Acad. Sci. U.S.A. **111**(21), 7546–7551 (2014).
22. Y. Wang, H. Sugimoto, S. Inampudi, A. Capretti, M. Fujii, and L. Dal Negro, "Broadband enhancement of local density of states using silicon-compatible hyperbolic metamaterials," Appl. Phys. Lett. **106**(24), 241105 (2015).
23. G. V. Naik, J. Liu, A. V. Kildishev, V. M. Shalaev, and A. Boltasseva, "Demonstration of Al:ZnO as a plasmonic component for near-infrared metamaterials," Proc. Natl. Acad. Sci. U.S.A. **109**(23), 8834–8838 (2012).
24. R. Stanley, "Plasmonics in the mid-infrared," Nat. Photonics **6**(7), 409–411 (2012).
25. H.-T. Chen, W. J. Padilla, J. M. O. Zide, A. C. Gossard, A. J. Taylor, and R. D. Averitt, "Active terahertz metamaterial devices," Nature **444**(7119), 597–600 (2006).
26. A. J. Hoffman, L. Alekseyev, S. S. Howard, K. J. Franz, D. Wasserman, V. A. Podolskiy, E. E. Narimanov, D. L. Sivco, and C. Gmachl, "Negative refraction in semiconductor metamaterials," Nat. Mater. **6**(12), 946–950 (2007).
27. E. Sachet, C. T. Shelton, J. S. Harris, B. E. Gaddy, D. L. Irving, S. Curtarolo, B. F. Donovan, P. E. Hopkins, P. A. Sharma, A. L. Sharma, J. Ihlefeld, S. Franzen, and J. P. Maria, "Dysprosium-doped cadmium oxide as a gateway material for mid-infrared plasmonics," Nat. Mater. **14**(4), 414–420 (2015).
28. J. Kim, G. V. Naik, N. K. Emani, U. Guler, and A. Boltasseva, "Plasmonic resonances in nanostructured transparent conducting oxide films," IEEE J. Sel. Top. Quantum Electron. **19**, 4601907 (2013).
29. C. Argyropoulos, P.-Y. Chen, G. D'Aguanno, N. Engheta, and A. Alù, "Boosting optical nonlinearities in ε-near-zero plasmonic channels," Phys. Rev. B **85**(4), 45129 (2012).
30. A. Alù and N. Engheta, "Achieving transparency with plasmonic and metamaterial coatings," Phys. Rev. E - Stat. Nonlinear," Soft Matter Phys. **72**, 1–9 (2005)..
31. M. G. Silveirinha, A. Alù, and N. Engheta, "Parallel-plate metamaterials for cloaking structures," Phys. Rev. E - Stat. Nonlinear. Soft Matter Phys. **75**, 1–16 (2007).
32. A. Alù and N. Engheta, "Cloaking a sensor," Phys. Rev. Lett. **102**(23), 233901 (2009).
33. S. Enoch, G. Tayeb, P. Sabouroux, N. Guérin, and P. Vincent, "A metamaterial for directive emission," Phys. Rev. Lett. **89**(21), 213902 (2002).
34. H. N. S. Krishnamoorthy, Z. Jacob, E. Narimanov, I. Kretzschmar, and V. M. Menon, "Topological transitions in metamaterials," Science **336**(6078), 205–209 (2012).
35. M. V. Klein and T. E. Furtak, *Optics*, 2. ed. (John Wiley & Sons, 1986).
36. A. K. Kulkarni, K. H. Schulz, T. S. Lim, and M. Khan, "Dependence of the sheet resistance of indium-tin-oxide thin films on grain size and grain orientation determined from X-ray diffraction techniques," Thin Solid Films **345**(2), 273–277 (1999).
37. W.-F. Wu, B.-S. Chiou, and S.-T. Hsieh, "Effect of sputtering power on the structural and optical properties of RF magnetron sputtered ITO films," Semicond. Sci. Technol. **9**(6), 1242–1249 (1994).
38. L. Meng and M. dos Santos, "Properties of indium tin oxide films prepared by rf reactive magnetron sputtering at different substrate temperature," Thin Solid Films **322**(1-2), 56–62 (1998).
39. L. Kerkache, A. Layadi, E. Dogheche, and D. Rémiens, "Physical properties of RF sputtered ITO thin films and annealing effect," J. Phys. D Appl. Phys. **39**(1), 184–189 (2006).
40. S. Takayama, T. Sugawara, A. Tanaka, and T. Himuro, "Indium tin oxide films with low resistivity and low internal stress," J. Vac. Sci. Technol. A Vacuum, Surfaces. Film. **21**, 1351–1354 (2003).
41. H. Han, J. W. Mayer, and T. L. Alford, "Effect of various annealing environments on electrical and optical properties of indium tin oxide on polyethylene napthalate," J. Appl. Phys. **99**(12), 123711 (2006).

1. Introduction

Conventional plasmonic materials such as noble metals have been widely used for plasmonic and metamaterial devices. However, metals feature high extinction losses in the visible and near-infrared (NIR) due to interband optical transitions and free carrier absorption. Moreover, they are not CMOS compatible and their optical permittivities show limited tunability. These

Optical Materials EXPRESS

facts severely limit practical device implementations on a Si platform. In recent years, Transparent Conductive Oxides (TCOs), including Indium Tin Oxide (ITO) and Al-doped ZnO (AZO), have gathered significant attention as a viable alternative to conventional noble metals for a variety of plasmonic device applications [1–7]. In particular, our group has recently demonstrated that post-deposition annealing in Ar and N_2 atmosphere results in a significant tailoring of the TCOs' optical and structural properties and also reduces their optical losses compared to Au and Ag in the NIR [8–10]. In addition, TCOs have a high melting points compared to noble metals and are chemically stable [11]. Currently, ITO and AZO are utilized as transparent electrical contacts in display technologies [12,13]. Moreover, the permittivity of TCOs can be flexibly engineered resulting in the Epsilon-Near-Zero (ENZ) behavior in a tunable spectral range that significantly enhances nonlinear optical generation processes [14–16]. Plasmonic TCOs have also recently been utilized to achieve enhanced electro-optical modulation [17–19], switching [20], enhanced light-matter interaction [21,22], and negative refraction [23].

In the mid-infrared spectral range, plasmonics technology offers an attractive approach to realize chemical sensing devices, quantum-well infrared detectors, and mid-infrared light sources [24]. However, the lack of compatibility with Si processing hampers the development of highly-integrated infrared-active devices based on Au and Ag. In addition, their materials dispersion properties can't be engineered. Heavily doped semiconductors can support plasmonic resonances in the terahertz [25] and long-wavelength mid-infrared [26] but the doping level needed to convert them into plasmonic materials in the technologically relevant 3-7 μm range is often prohibitively large. Materials such as dysprosium-doped cadmium oxide grown by molecular beam epitaxy (MBE) have been recently developed to exhibit tunable mid-infrared optical properties with a defect engineering approach [27].

In the present work, we show an alternative, Si-compatible and largely scalable approach based on ITO thin films post-processing by thermal annealing treatments in oxygen (O_2) atmosphere. We characterize the synthesized materials using Fourier transform infrared (FTIR) spectroscopy and demonstrate that tunability of their optical properties and significantly reduced optical losses can be extended to the mid-infrared. In addition, we fabricate two-dimensional (2D) periodic arrays of ITO discs by electron-beam lithography (EBL) and experimentally demonstrate that their size-dependent plasmonic scattering resonances can be tuned from λ = 5 to 10 μm by varying the diameters of the disks. Our findings pave the way to the development of scalable and cost-effective mid-infrared devices for active plasmonic sensing and spectroscopy on a silicon platform.

2. Sample deposition and characterization

The permittivity $\varepsilon(\omega)$ of ITO materials can be described by the Drude-Sommerfeld model [28]:

$$\varepsilon(\omega) = \varepsilon_1(\omega) + i\varepsilon_2(\omega) = \varepsilon_\infty - \frac{\omega_p^2}{\omega^2 + i\Gamma\omega} \tag{1}$$

where ε_∞ is the high frequency limit of $\varepsilon(\omega)$, ω_p is the plasma frequency and Γ is the charge carrier collision rate. The plasma frequency can be expressed as:

$$\omega_p^2 = \frac{ne^2}{\varepsilon_0 m^*} \tag{2}$$

where e is elementary charge, n is the carrier concentration, m* is the effective mass of electron and ε_0 is the permittivity of free space.

In order to achieve negative permittivity, a free career concentration of the order of 10^{20}-10^{22} cm^{-3} is needed. The wavelength at which the real part of the permittivity, ε_1, is

Optical Materials EXPRESS

approximately zero is known as the epsilon-near-zero (ENZ) wavelength, λ_{ENZ}. Typically the intrinsic doping of ITO is large so that the ENZ point occurs in the near-infrared region [3,10], which enables applications such as nonlinear optics [14,15,29], optical cloaking [30–32], and controlling the radiation patterns of dipolar emitters embedded in the material [33,34]. The challenge is to reduce the doping level so that the ENZ point can shift to the mid-infrared.

In this paper we demonstrate a convenient strategy to achieve this goal. In particular, by systematically studying the optical dispersion of a large number of ITO thin films deposited by magnetron sputtering, we show that post-deposition annealing in oxygen atmosphere allows for tuning the λ_{ENZ} well into the mid-IR spectral range. We notice that despite the large skin depth of ITO in the mid-IR range compared to noble metals, the plasmonic quality factor $Q = \mathrm{Re}\{\varepsilon\}/\mathrm{Im}\{\varepsilon\}$ (i.e., the ratio of the real and imaginary parts of the complex permittivity) of our synthesized ITO materials is comparable to that of noble metals (at 10 μm, the quality factor for Au, Al and our synthesized ITO are all around 2.0), but within a fully Si-compatible materials approach. We fabricate ITO micro-disk devices and observe size-dependent plasmonic responses in the mid-IR.

2.1 Optical properties of ITO

ITO thin films were deposited using RF magnetron sputtering using a Denton Discovery 18 confocal-target system, with an ITO (99.99% purity) target in Ar atmosphere at room temperature. The sputtering power was varied from 40 to 200 W. The base pressure was 1.0×10^{-7} Torr and the Ar gas flow was kept at 12 sccm. The thickness of all the fabricated ITO samples was kept constant at ~209 nm, irrespective of the deposition conditions.

We conducted post-deposition annealing using a Mellen thermal furnace, which resulted in a large tunability of the measured optical dispersion of ITO in the NIR and mid-IR spectra. After annealing, the film thickness remains unchanged (thickness error: ± 5 nm), as independently verified by spectroscopic ellipsometry and surface profilometry. Annealing processes were performed in Ar or O_2 gas atmosphere under atmospheric pressure at temperatures between 350 and 750 °C for 1 hour. Table 1 summarizes the sputtering power and annealing conditions for all the ITO samples.

Table 1. Sputtering and annealing parameters of ITO thin films on Si substrates

Sputtering Power (W)	Thickness (nm)	λ_{ENZ} (nm)	ε_2 @ λ_{ENZ}	Annealing Temp. (°C)	Annealing gas
200	209	1830	0.85	As Deposited	
200	209	1150	0.33	750	Ar
200	209	3001	1.47	750	O_2
100	209	1866	0.61	As Deposited	
100	209	2505	4.11	350	O_2
100	209	2742	4	550	O_2
100	209	3230	1.18	750	O_2
80	209	3430	2.05	750	O_2
60	209	3700	2.94	750	O_2
40	209	4270	2.96	750	O_2

The infrared optical properties of the ITO films were measured using a Fourier Transform Infrared (FTIR) spectrometer (Bruker Scientific Vertex 70v), which is equipped with a TE-cooled InGaAs detector (covering λ = 1 to 2.5 μm) and a liquid-nitrogen-cooled mercury-cadmium-telluride detector (covering λ = 2.5 to 16 μm). The reflectance spectra of the thin films were measured using a silver mirror as a reference. The measured data were fit by considering thin film interference and the materials dispersion of ITO characterized by the

Optical Materials EXPRESS

Drude-Sommerfeld model (Eq. (1)) [35]. The film thickness was taken from spectroscopic ellipsometry measurements as 209 nm, leaving the fitting parameters to be (1) the background permittivity, ϵ_∞, (2) the plasma frequency, ω_p, and (3) the scattering rate, Γ. Figure 1 shows the results of fitting a few FTIR reflection spectra.

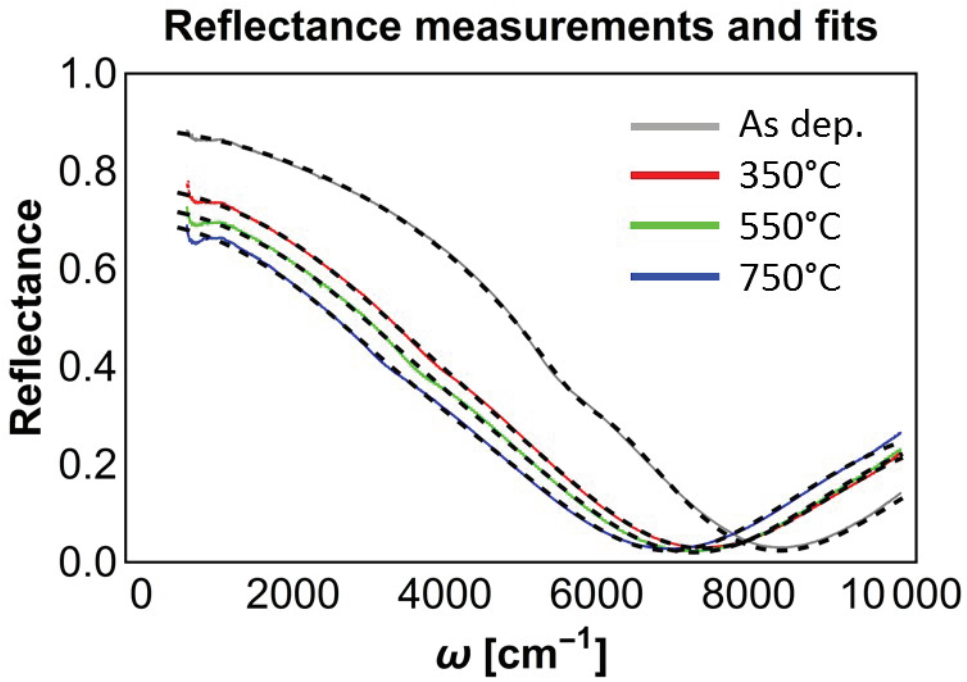

Fig. 1. Examples of FTIR reflectance spectra (solid) and Drude model fit (dashed), for the as deposited sample (grey), sample annealed at 350 °C for 1h (red), sample annealed at 550 °C for 1h (green) and sample annealed at 750 °C for 1h (blue).

2.1.1 Effect of sputtering power

In order to investigate the tunability of the dispersion properties of ITO thin films in the mid-IR, we first measured the permittivity of ITO samples deposited with different sputtering powers. Upon deposition, all ITO samples were annealed at 750 °C in O_2 for 1 hour. The sputtering conditions are listed in Table 2.

Table 2. Effects of sputtering power on optical dispersion of ITO thin films deposited on Si substrates

Sputtering Power (W)	Thickness(nm)	λ_{ENZ} (nm)	ε_2 @ λ_{ENZ}
200	209	3001	1.47
100	209	3230	1.18
80	209	3430	2.05
60	209	3700	2.94
40	209	4270	2.96

Figure 2 shows the experimentally measured optical permittivity data for ITO samples annealed in O_2, which illustrate the effect of the sputtering power on the real (ε_1) and imaginary (ε_2) parts of the complex permittivity. Consistent with our previous publications [8], oxygen annealing of ITO leads to a reduction in the density of oxygen vacancies (corresponding to reduced free carriers in ITO materials) that shifts the λ_{ENZ} from the near-IR (when annealed in Ar/N_2) into the mid-IR range. Our data demonstrates that the λ_{ENZ} of the

Optical Materials EXPRESS

ITO samples can be largely tuned in the 3000-4300 nm range by varying the sputtering power. As the sputtering power is decreased, the λ_{ENZ} is increased, which provides a convenient strategy to engineer the dispersion properties of ITO in mid-IR when annealing in O_2.

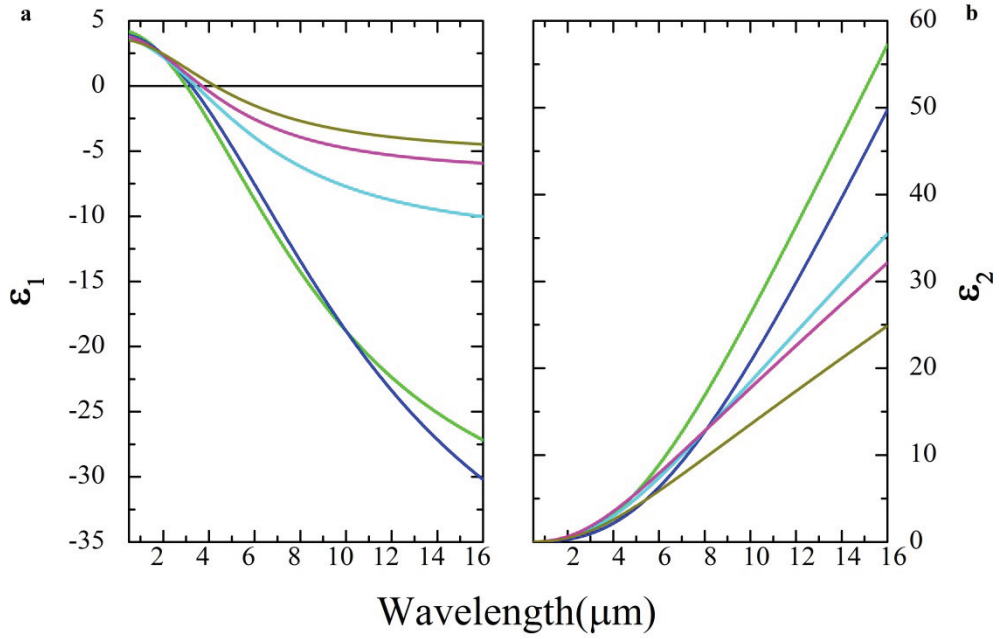

Fig. 2. Real (a) and imaginary (b) part of permittivity of ITO samples on Si substrate sputtered at different power: 200W (green), 100W (blue), 80W (cyan), 60W (magenta), 40W (dark yellow). All samples are annealed at 750 ˚C in O_2 for 1h.

Figure 3 summarizes the λ_{ENZ} and ε_2 data as a function of sputtering power for our ITO samples. The significant effect of the sputtering power on the optical properties of ITO thin films is clearly displayed. In particular, we notice that as the sputtering power is increased, both the λ_{ENZ} and ε_2 decrease. This is due to the decreased oxygen contents in the fabricated ITO as sputtering power increases. It is well understood in other literature that as the sputtering power increases, the preferred orientation of the ITO film changes from (222) to (400). Therefore, the lattice constant of the ITO film increases initially as sputtering power increases and then decreases with further increase of sputtering power [36,37]. We note that the imaginary part of the permittivity ε_2 at the λ_{ENZ} varies in the range 1.18–4.11 for ITO (see Table 1), which is larger than the ε_2 obtained for ITO samples annealed in Ar. We ascribe this difference to the decreased density of grain boundaries of the ITO samples annealed in Ar compared to those annealed in O_2. The ITO samples annealed in Argon has smaller resistivity than those annealed in oxygen, thus they have smaller optical loss ε_2 [38–41].

Optical Materials EXPRESS

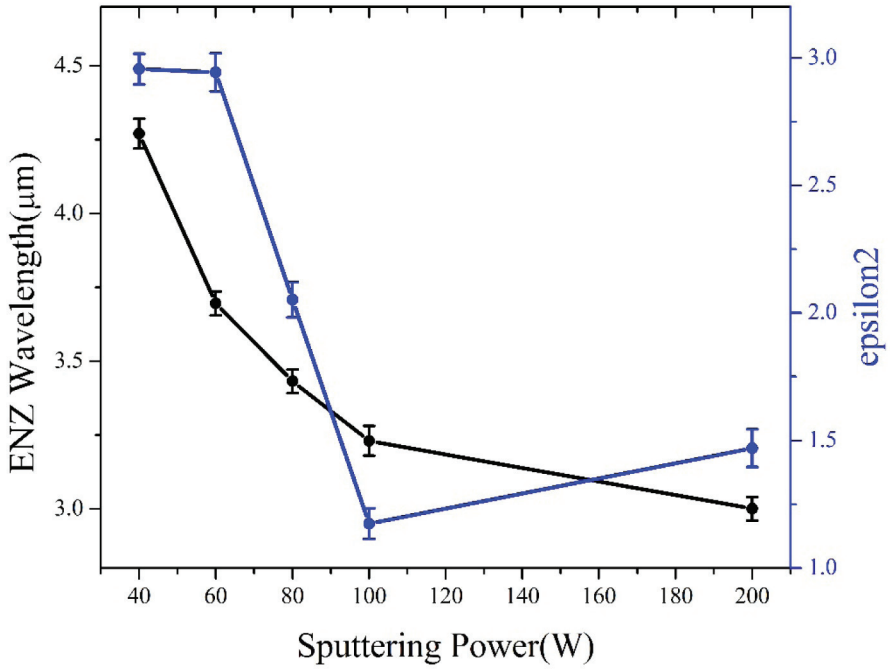

Fig. 3. λ_{ENZ} (black curves on left axis with error bar) and ε_2 (blue curves on right axis with error bar) as a function of the sputtering power. All samples are annealed at 750 °C in O_2 for 1h. The error bar is estimated based on ITO samples sputtered and annealed at same condition. For each sputtering power, 5 ITO samples are characterized to estimate the error bar.

2.1.2 Tunability of the ENZ condition of ITO from the near-IR to mid-IR spectral range

In order to demonstrate the tunability of the λ_{ENZ} of ITO thin films from the near-IR to the mid-IR spectrum, the measured permittivity data of samples deposited and annealed at different sputtering powers and ambient gases are reported in Fig. 4. These samples feature λ_{ENZ} in the range between 1150 nm to 4270 nm, demonstrating that the ENZ condition can be largely tailored by post-deposition thermal annealing processes. Notice that the as-deposited samples and the samples annealed at 750 °C for 1h in Ar show the ENZ condition in the near-IR range (1150-2000 nm). On the contrary, samples annealed in oxygen at 750 °C for 1h and at different sputtering powers demonstrate a tunable ENZ condition in the mid-IR range (3000-4300 nm). All the sputtering and annealing conditions of ITO samples in Fig. 4 are summarized in Table 1.

Optical Materials EXPRESS

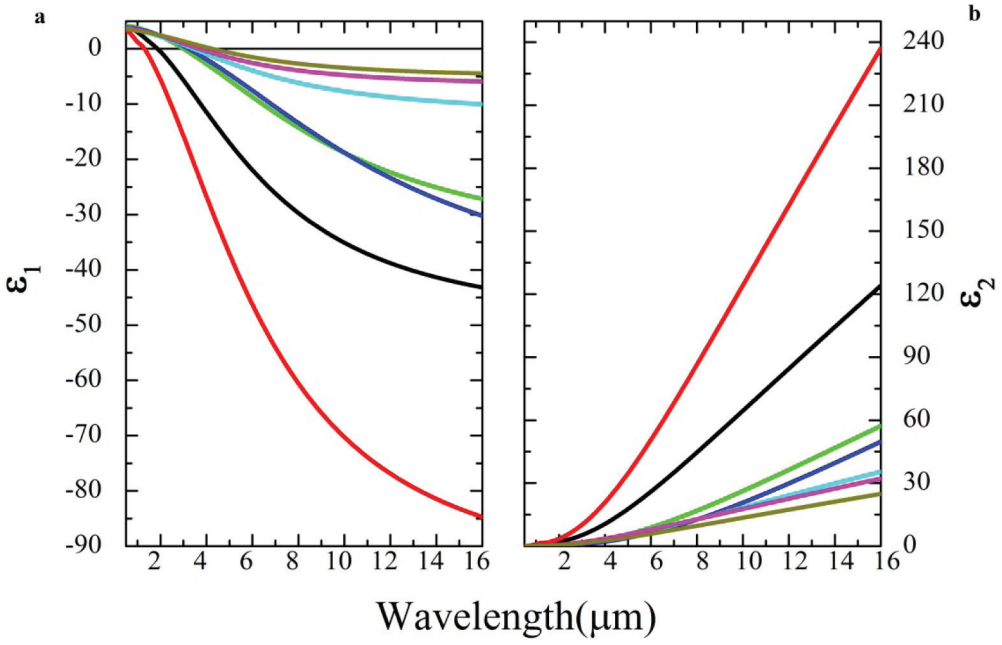

Fig. 4. Real (a) and imaginary (b) parts of permittivity of ITO thin films deposited on Si substrates with annealing conditions and sputtering powers: As-dep_200W (black), 750 ˚C Ar 1h_200W (red), 750 ˚C O_2 1h_200W (green), 750 ˚C O_2 1h_100W (blue), 750 ˚C O_2 1h_80W (cyan), 750 ˚C O_2 1h_60W (magenta), and 750 ˚C O_2 1h_40W (dark yellow).

2.1.3. Effect of annealing temperature

The effect of growth temperature on the optical properties of ITO has been previously reported [11,28]. Here we focus on understanding the role of the annealing temperature on the dispersion properties of ITO by performing post-deposition annealing in O_2 atmosphere between 350 and 750 °C for 1 hour, as summarized in Table 3.

Table 3. Effect of annealing temperatures on optical dispersion of ITO

Sputtering Power (W)	Thickness(nm)	λ_{ENZ} (nm)	ε_2 @ λ_{ENZ}	Annealing Temp. (°C)	Annealing Gas
100	209	1866	0.61	As Deposited	
100	209	2505	4.11	350	O_2
100	209	2742	4	550	O_2
100	209	3230	1.18	750	O_2

Figure 5 shows the permittivity of ITO samples annealed at different temperature. As the annealing temperature increases, the optical losses decrease and the λ_{ENZ} increases from 2500 to 3200 nm, as also shown in Fig. 6. This behavior is very different from what previously reported in [8] when ITO was annealed in Ar/N_2, which resulted in a decrease of both λ_{ENZ} and ε_2 when the annealing temperature was increased. Our results suggest that oxygen vacancies play a key role in reducing the density of free carriers in ITO, thus shifting the λ_{ENZ} from the near-IR (when annealed in Ar) into the mid-IR spectrum.

Optical Materials EXPRESS

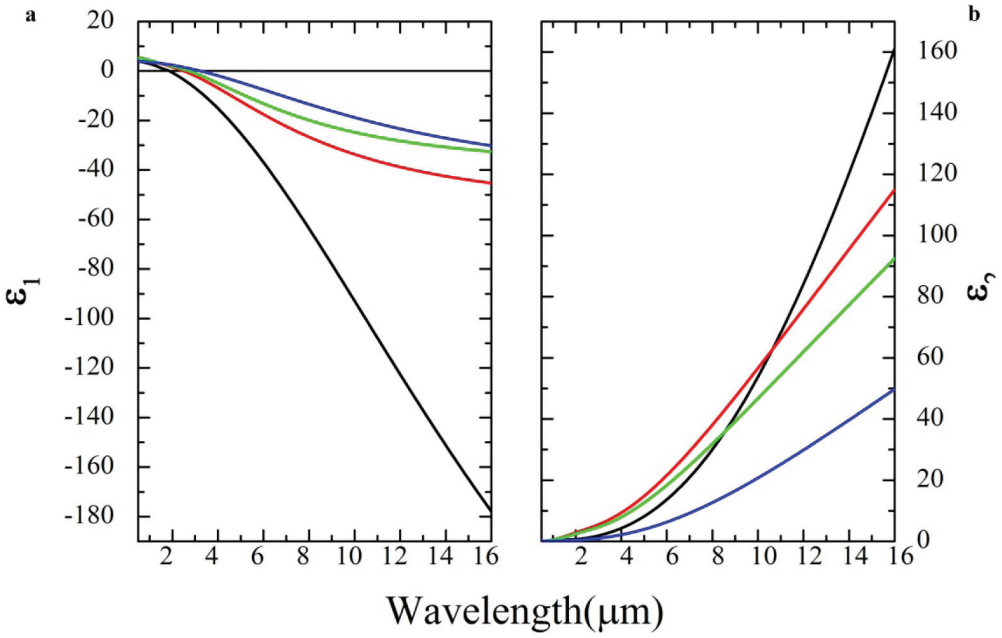

Fig. 5. Real (a) and imaginary (b) parts of permittivity of ITO samples deposited on Si substrates and annealed at different temperatures: As deposited (black), 350 °C (red), 550 °C (green), 750 °C (blue). The annealing was performed in O_2 atmosphere for 1h for all samples.

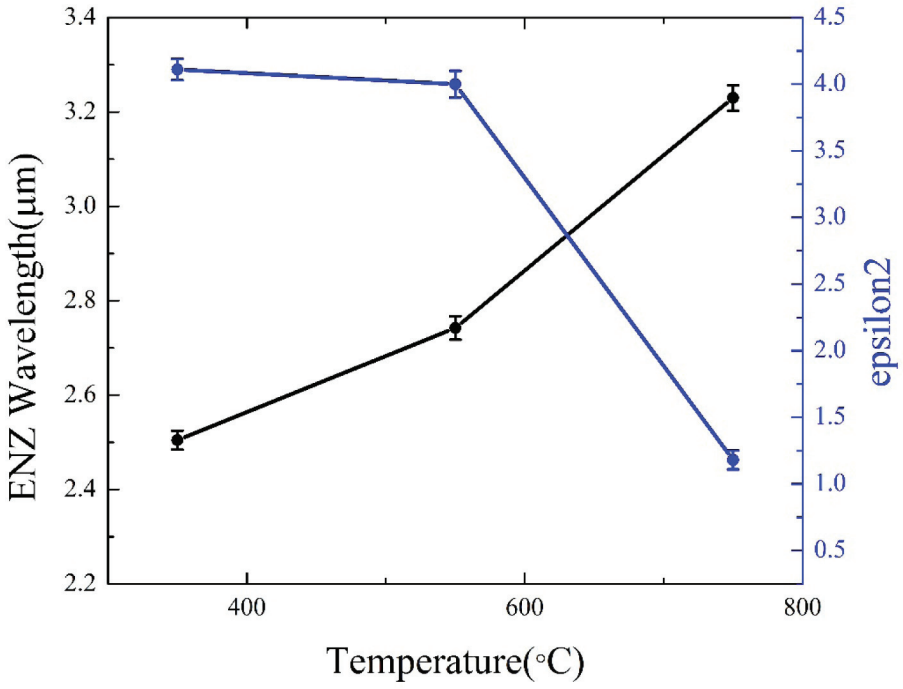

Fig. 6. λ_{ENZ} (black curves on left axis with error bar) and ε_2 (blue curves on right axis with error bar) as a function of the annealing temperature. All samples are annealed in O_2 for 1h. The error bar is estimated based on ITO samples sputtered and annealed at same condition. For each annealing temperature, 5 ITO samples are characterized to estimate the error bar.

Optical Materials EXPRESS

3. Tunable plasmonic resonances of ITO micro-disks

ITO annealed in O_2 can be used as a tunable plasmonic material in the mid-IR. We fabricated 2D ITO disk arrays with diameters in the range of 1-5 μm on CaF_2 substrates (Fig. 7 (a)). We demonstrate that the position of the plasmon resonance of the micro-disks can be shifted in the mid-IR by changing the diameter of the discs, in good agreement with our electromagnetic simulation results.

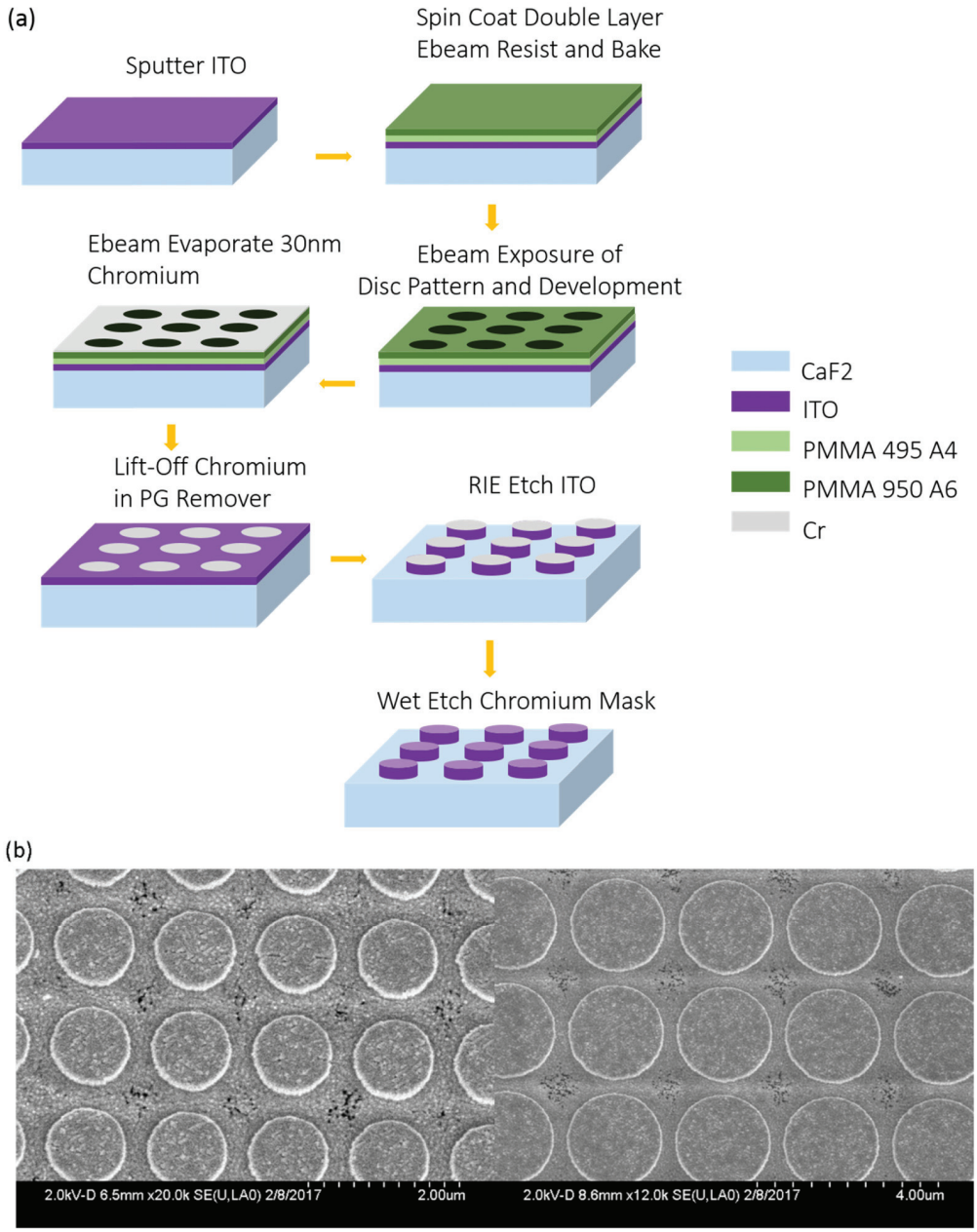

Fig. 7. (a) Schematic showing the process of fabricating arrays of ITO discs. (b) Representative SEM images of fabricated ITO disk arrays with diameters of 1 μm (left) and 2 μm (right).

Optical Materials EXPRESS

Specifically, the micro-discs were fabricated by first depositing 280-nm ITO thin films using RF magnetron sputtering on CaF_2 substrates at room temperature. The CaF_2 substrates were chosen because of their transparency in the mid-IR spectrum. A double layer resist (PMMA 495 A4 and 950 A2) was spun on the wafers and disc array patterns were written with electron beam lithography (JEOL JBX-6300FS) with a dose of 800 μ C/cm^2 at a current of 200 pA. The sample was developed in IPA:DI (3:1) for 2 minutes followed by the deposition of a 70-nm chromium mask using electron beam evaporation. After lifting off the mask in Remover 1165, the disc array patterns were transferred to ITO by plasma etching (RIE, Plasma-Therm, model 790) in a mixture of CH_4 and H_2. Finally, the chromium mask was removed by wet etching in Transene 1020. After that, the ITO disk arrays were annealed at 750 $^{\circ}$C in O_2 for 1 hour. Figure 7(b) shows Scanning Electron Microscopy (SEM) images of fabricated ITO arrays with diameters of 1 μm and 2 μm.

A commercial simulator (Lumerical) based on the finite-difference time-domain (FDTD) method is used to calculate reflectance spectra of micro-disc arrays. The intensity of the reflected infrared light is computed under normal incidence condition. In Fig. 8(a), we present calculated reflectance spectra for ITO disks with diameters ranging from 1 μm up to 5 μm. In Fig. 8(b), measured FTIR spectra are shown. The results clearly indicate the excitation of a size-dependent plasmon resonance in the ITO disks, with a shift of the plasmonic resonance peak that follows the theoretical predictions. In particular, as the diameter of the ITO disks increases, the reflectance spectral peak shifts to longer wavelengths. However, the simulation results for ITO disks with diameters of 4 μm and 5 μm feature a larger peak shift and a broader spectrum compared to the experimental results. These differences are attributed to fabrication imperfections (residual ITO that covers the CaF_2 substrates, over-etching in the regions that are between adjacent four micro-discs). Furthermore, we notice that the small dips in the calculated reflectance spectra (Fig. 8(a)) of disks with diameters of 4 μm and 5 μm correspond to the excitation of grating resonances in a perfectly periodic structure (FDTD simulations were conducted using periodic boundary conditions), and cannot be expected in the fabricated finite-size samples.

In Fig. 8(c) and (d) we show two representative electric-field distributions across the middle height of the disks at the peak of the simulated reflectance spectra (Fig. 8(a)): λ = 6.1 μm for ITO disks with 1 μm diameter and λ = 12.0 μm for ITO discs with 5 μm diameter. At λ = 6.1 μm, the field distribution is predominantly due to a dipolar response induced at a wavelength significantly larger than the disk size. Compared to the distribution in Fig. 8(d), there is more field inside the disks in Fig. 8 (c) due to the smaller value of the imaginary part of ITO permittivity, which makes ITO at this wavelength behave as a non-ideal metal. In contrast, as shown in Fig. 8(d), a dipolar field distribution is induced at the edges of the 5-μm disk at the peak wavelength of reflectance (λ = 12.0 μm) where a much larger imaginary part of the ITO permittivity makes the ITO material more metallic in nature. These findings demonstrate that ITO thin films with engineered dispersion support strongly confined plasmonic modes and are ideally suited for the fabrication of plasmonic structures with largely tunable spectral resonances across the mid-IR range.

Optical Materials EXPRESS

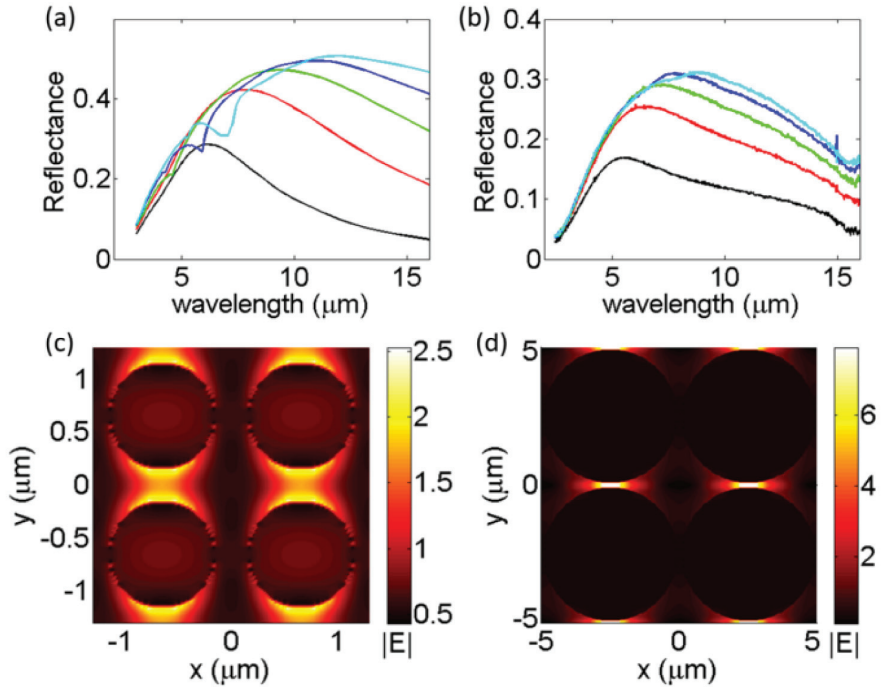

Fig. 8. (a) FDTD simulations of the reflectance spectra of ITO disk arrays as a function of disk diameter: 1 μm (black), 2 μm (red), 3 μm (green), 4 μm (blue), 5 μm (cyan). All ITO discs have a height of 280 nm. (b) Measured reflectance spectra of ITO disk arrays patterned on CaF_2 substrates with different disk diameters: 1 μm (black), 2 μm (red), 3 μm (green), 4 μm (blue), 5 μm (cyan). (c) and (d) are field distributions inside and around the 1 μm and 5 μm ITO disks at λ = 6.1 μm and 12.0 μm, respectively (peaks of reflectance spectra).

4. Conclusion

We establish the critical roles of sputtering power, annealing in O_2 atmosphere, and annealing temperature in tuning the dispersion properties in ITO thin films in the mid-infrared spectrum. We experimentally demonstrate wide tuning of the plasmonic resonance of ITO micro-disks from λ = 5 to 10 μm. The engineered ITO platform shows the critical importance of the fabrication conditions in achieving the wide tunability of optical properties that is needed for the development of scalable and cost-effective mid-infrared devices for active metamaterials and plasmonic devices on the widespread silicon platform.

Funding

National Science Foundation (ECCS 1541678, ECCS 1643118); AFOSR MURI (FA9550-14-1-0389, DGE-1069240); U.S. Department of Energy, Office of Basic Energy Sciences (DE-SC0012704).

Acknowledgments

This work was supported by the NSF EAGER program "Engineering light-matter interaction via topological phase transitions in photonic heterostructures with aperiodic order" under Award No. ECCS 1541678, the NSF EAGER program "Enhanced Solar Energy Conversion by Ultra-slow Photon Sub-diffusion in Aperiodic Media" under Award No. ECCS 1643118, and AFOSR MURI (Multidisciplinary University Research Initiative) FA9550-14-1-0389: "Active Metasurfaces for Advanced Wavefront Engineering and Waveguiding". Adam Overvig is supported by an NSF IGERT award under Award Number DGE-1069240.

Optical Materials EXPRESS

Research was carried out in part at the Center for Functional Nanomaterials, Brookhaven National Laboratory, which is supported by the U.S. Department of Energy, Office of Basic Energy Sciences, under Contract No. DE-SC0012704.